Fabrication and characterization of dimethylammonium added perovskite solar cells

THE UNIVERSITY OF SHIGA PREFECTURE [1]The University of Shiga Prefecture, OSAKA GAS CHEMICALS [2]Osaka Gas Chemicals Co. Ltd.

Haruto Shimada[1], Takeo Oku[1], Atsushi Suzuki[1], Tomoharu Tachikawa[2], Tomoya Hasegawa[2], and Sakiko Fukunishi[2]

CIC 2025 Conference

Perovskite solar cells

・Next-generation solar cells to replace Si-based solar cells

Advantage

・Flexible structure

・Superior photoelectric conversion properties

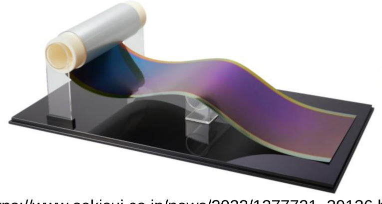

Problem

・Low stability

・Small cell

https://www.sekisui.co.jp/news/2022/1377721_39136.html

Structure of perovskite

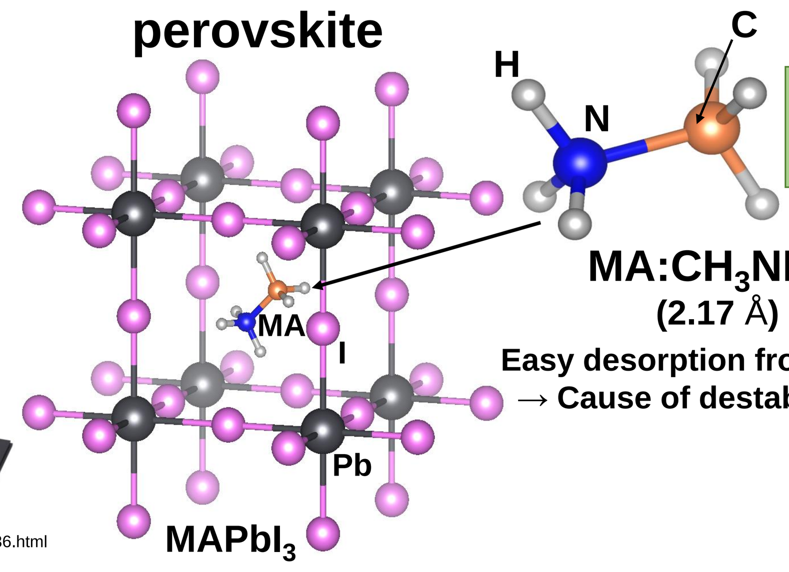

MAPbI$_3$

MA:$CH_3NH_3^+$ (2.17 Å)

Easy desorption from crystal → Cause of destabilization

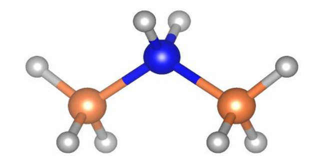

DMA:$CH_3NH_2CH_3^+$ (2.72 Å)

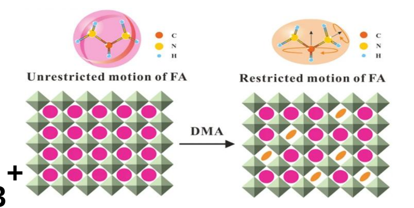

W. C. Qiao, et al. NPG Asia Mater. 14, 49 (2022).

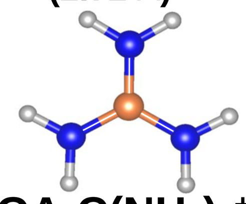

GA:$C(NH_2)_3^+$ (2.78 Å)

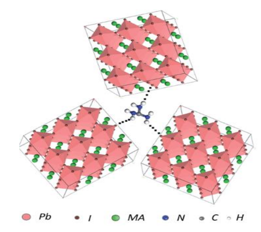

X Hou, et al. J. Mater. Chem. A, 5, 7314, 49 (2017).

Role of DMA/GA

・DMA

・Stabilization of PbI$_6$ structure

・Photovoltaic property improvement

・GA

・Defect suppression

・Thermal stability improvement

Method

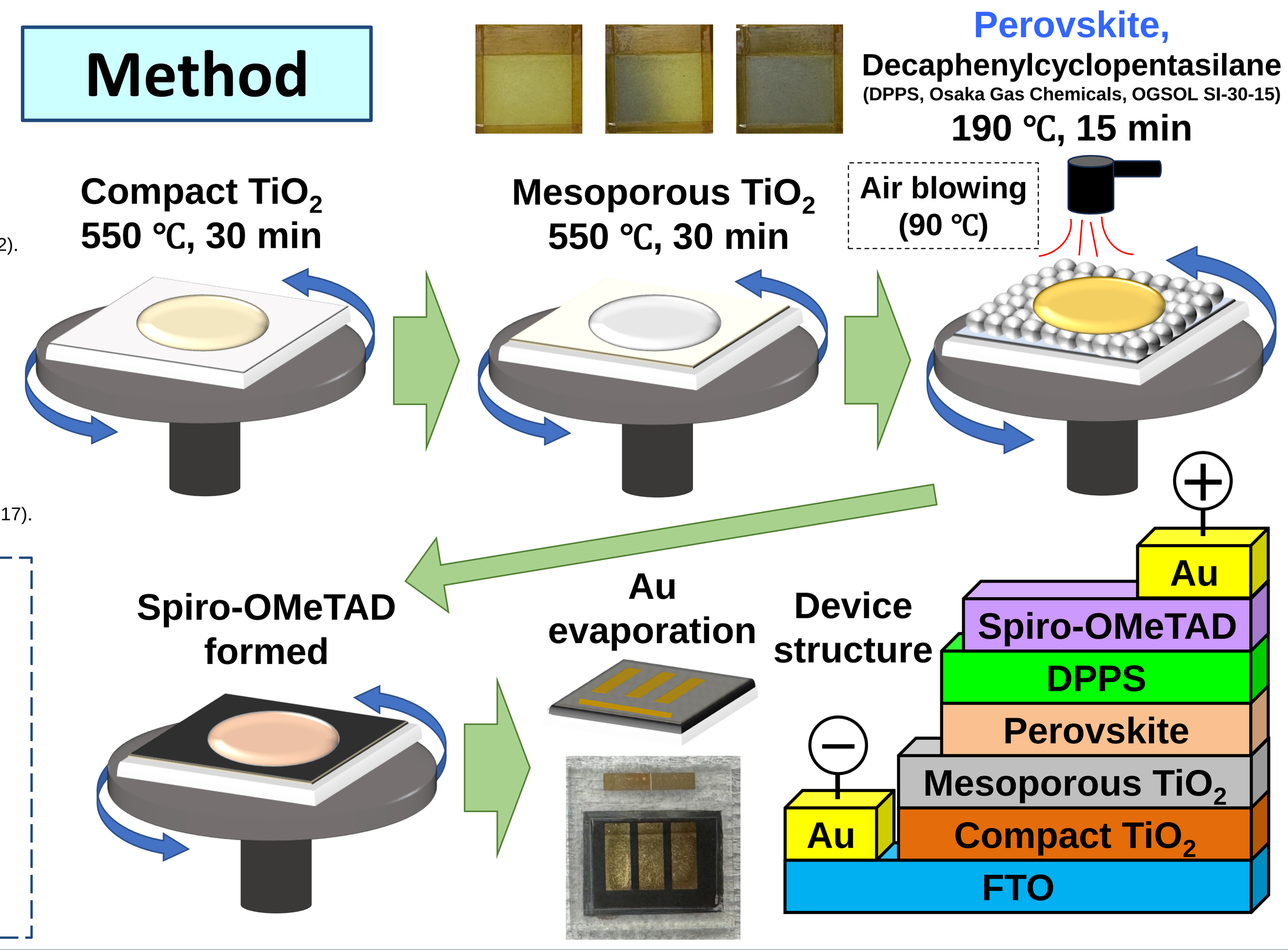

Purpose

・To investigate the effects of adding DMA to MAPbI$_3$ solar cells

・DMA/GA co-added device fabrication to improve stability and photoelectric conversion properties

Results and discussion

DMA addition

J-V characteristic | XRD patterns | Changes of η | Dark J-V

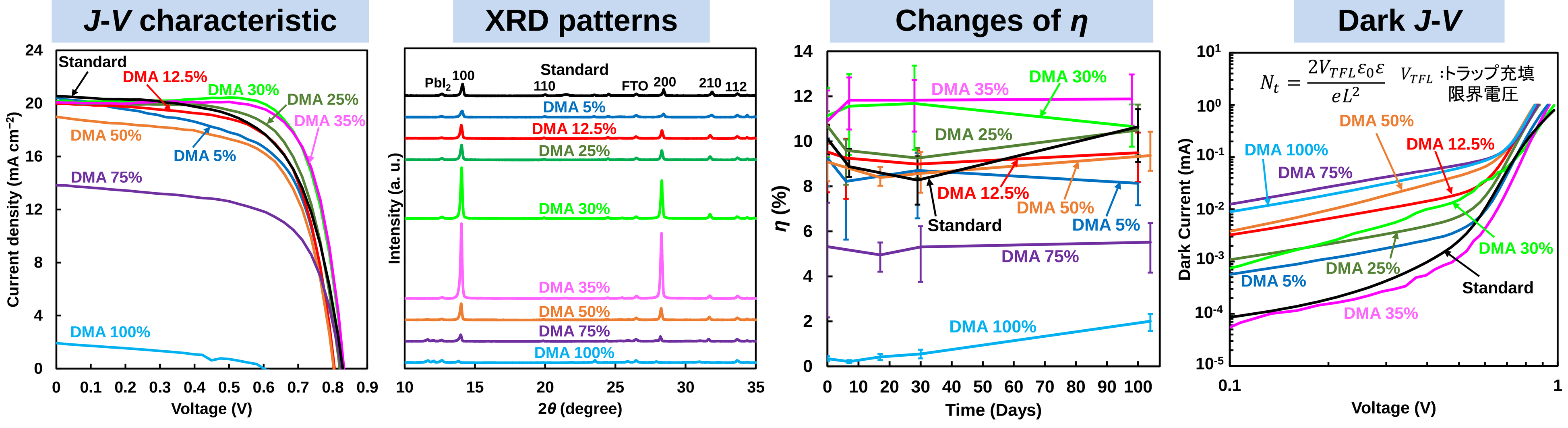

$N_t = \frac{2V_{TFL}\varepsilon_0\varepsilon}{eL^2}$

DMA/GA co-addition

J-V characteristic | EQE spectrum | XRD patterns | Changes of η

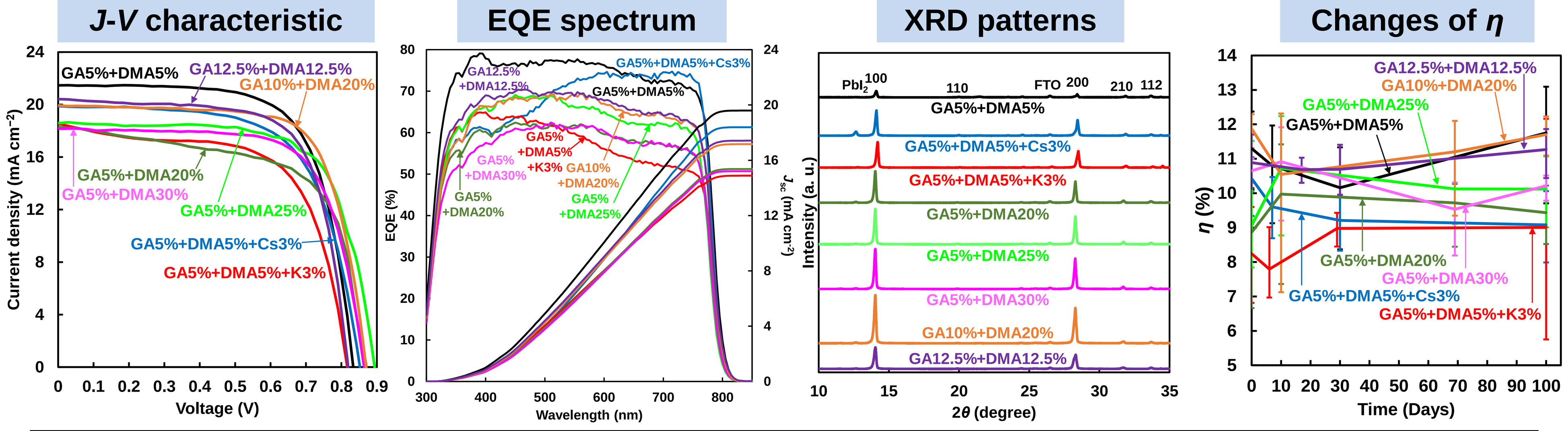

Devices	J_{SC} (mA cm^{-2})	V_{OC} (V)	FF	R_S (Ω cm^2)	η (%)	η_{ave} (%)	t-factor	Lattice constant (Å)	Crystallite size (Å)	I_{100} / I_{210}
Standard	20.5	0.829	0.628	3.57	10.7	10.1	0.911	6.271(1)	525	2.58
DMA 12.5%	20.0	0.805	0.668	1.65	10.7	9.53	0.926	6.298(3)	557	3.88
DMA 25%	20.1	0.820	0.688	2.14	11.3	10.7	0.940	6.302(1)	573	4.06
DMA 30%	20.2	0.832	0.738	1.21	12.4	11.1	0.946	6.302(1)	668	10.6
DMA 35%	20.1	0.832	0.733	1.41	12.3	10.9	0.952	6.305(0)	752	25.3
DMA 50%	19.0	0.803	0.649	1.91	9.89	9.08	0.969	6.312(0)	633	5.05
GA 5% DMA 5%	21.5	0.833	0.692	2.59	12.4	11.3	0.924	6.270(1)	557	4.25
GA 5% DMA 5% Cs 3%	19.9	0.852	0.651	4.31	11.0	10.4	0.922	6.263(1)	589	13.3
GA 5% DMA 25%	18.6	0.893	0.693	3.36	11.5	9.06	0.947	6.305(1)	689	14.3
GA 5% DMA 30%	18.2	0.864	0.702	3.41	11.0	10.6	0.952	6.307(0)	658	17.4
GA 10% DMA 20%	19.9	0.870	0.715	2.89	12.4	11.4	0.947	6.304(0)	591	26.4
GA 12.5% DMA 12.5%	20.4	0.818	0.701	1.44	11.7	10.9	0.942	6.300(0)	503	18.3

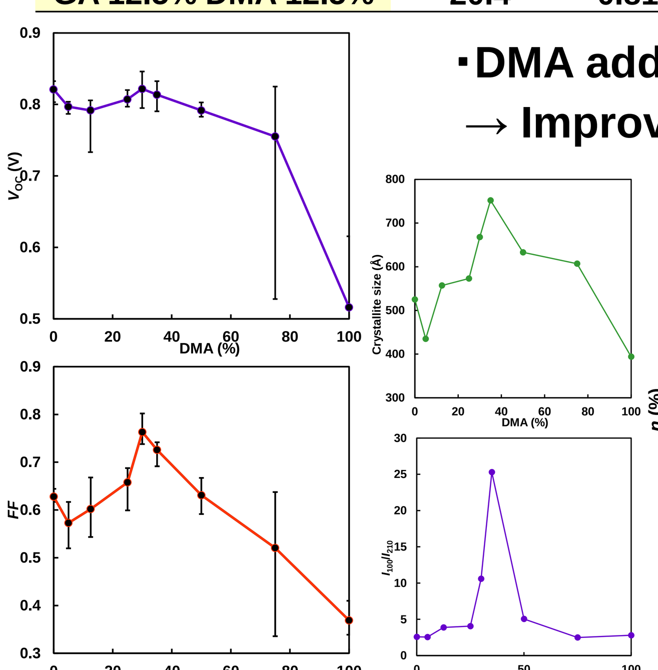

・DMA addition (~35%)

→ Improved V_{OC} and FF

・DMA/GA co-addition

→ Large crystallite size and high I_{100}/I_{210}

⇒ Improved J_{SC} and FF

Tolerance factor

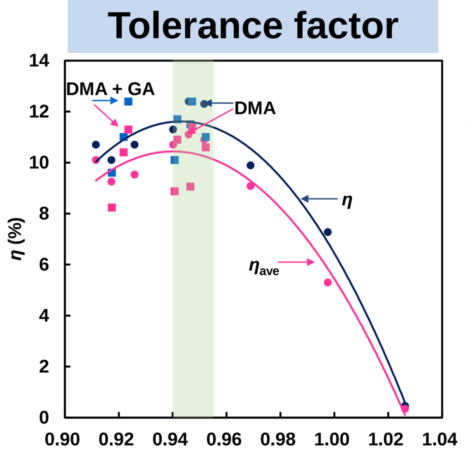

・DMA/GA total 25~35% addition

t = 0.911(MAPbI$_3$) → 0.940~0.955

$$t = \frac{r_A + r_x}{\sqrt{2}\,(r_B + r_x)}$$ r : Ionic radius

→ Cubic crystals with smaller distortion

⇒ More stable crystal structure

SEM EDS

MAPbI$_3$

MA$_{0.70}$DMA$_{0.30}$PbI$_3$

MA$_{0.70}$DMA$_{0.20}$GA$_{0.10}$PbI$_3$

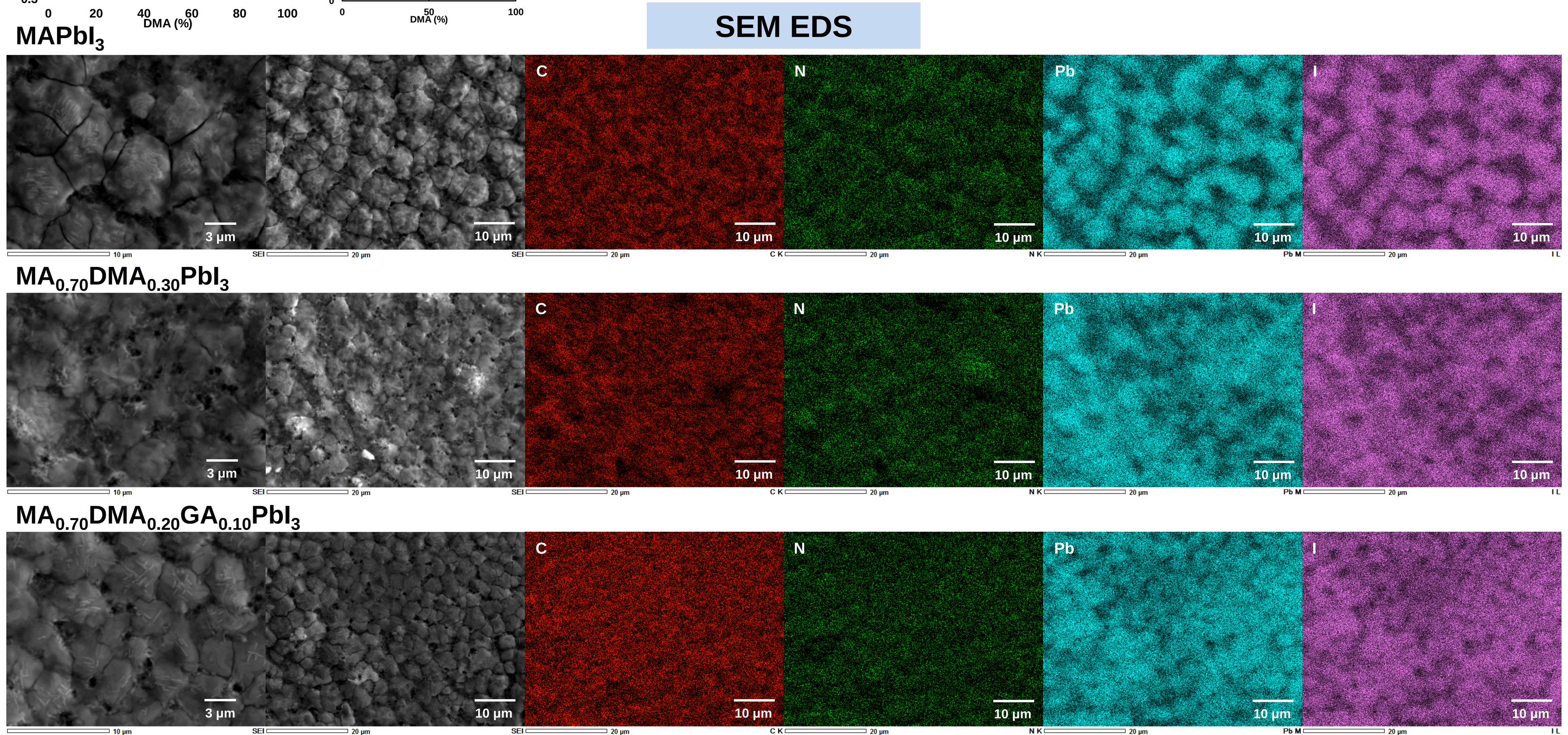

AFM

MA$_{0.70}$DMA$_{0.30}$PbI$_3$

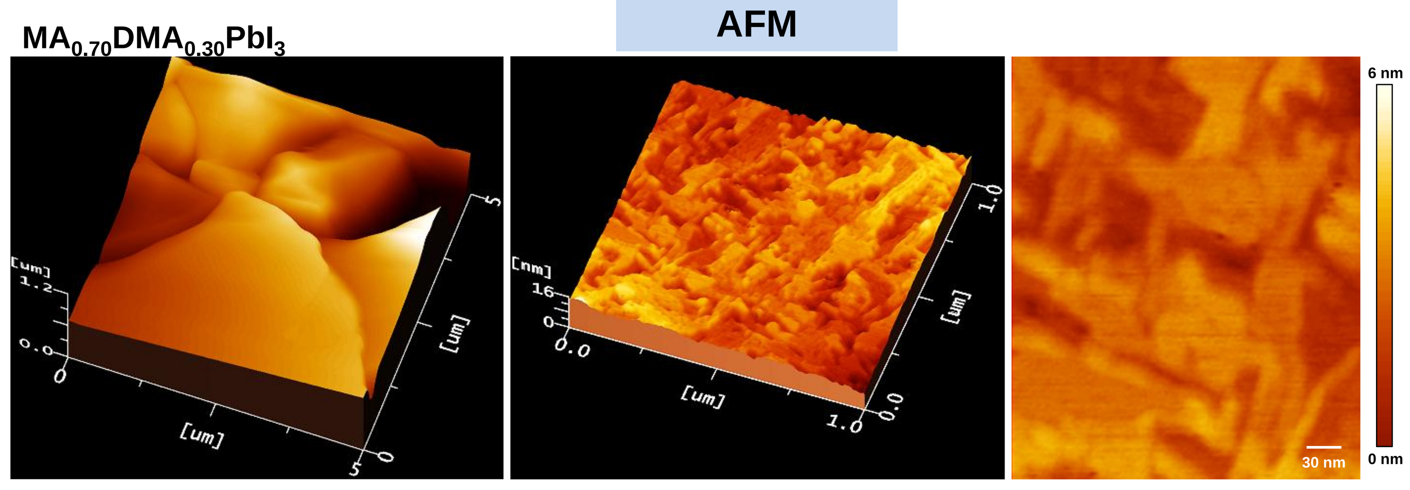

FTIR

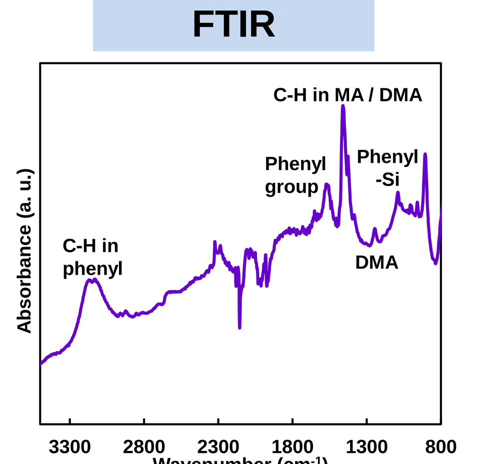

First principle calculation

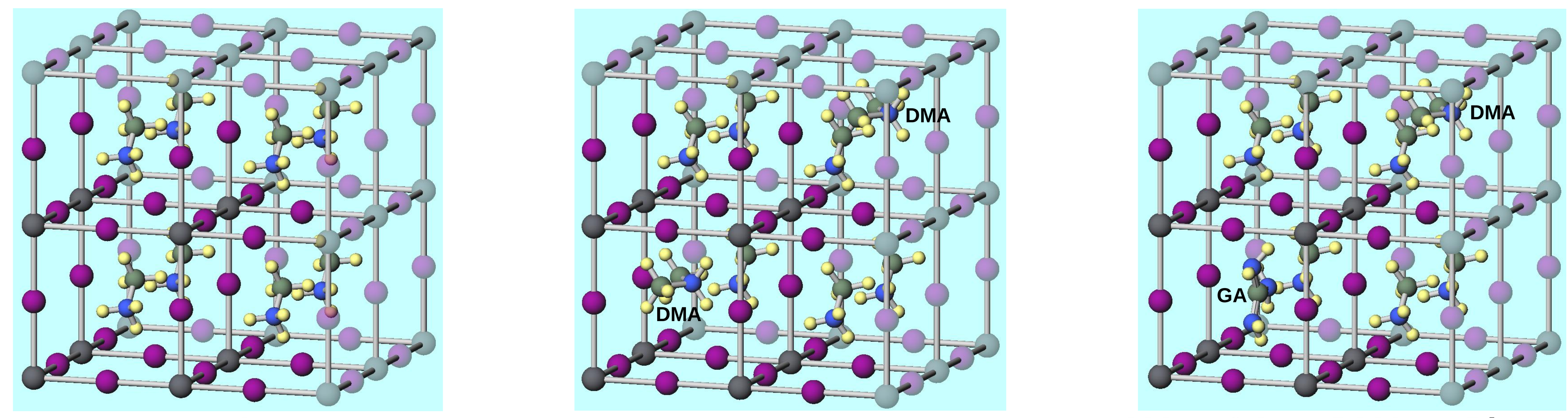

MAPbI$_3$ | MA$_{0.75}$DMA$_{0.25}$PbI$_3$ | MA$_{0.75}$GA$_{0.125}$DMA$_{0.125}$PbI$_3$

Band structures・pDOS

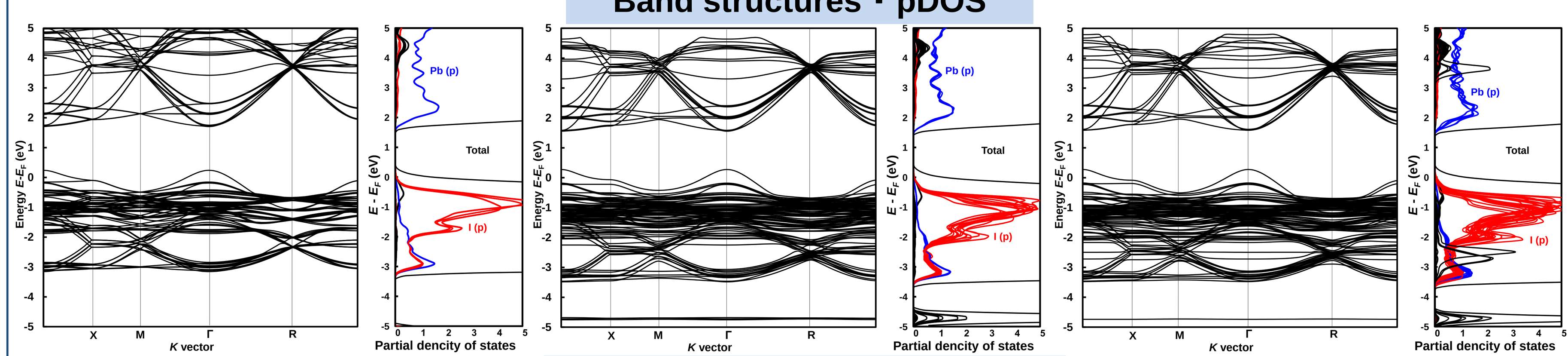

Electron density distributions

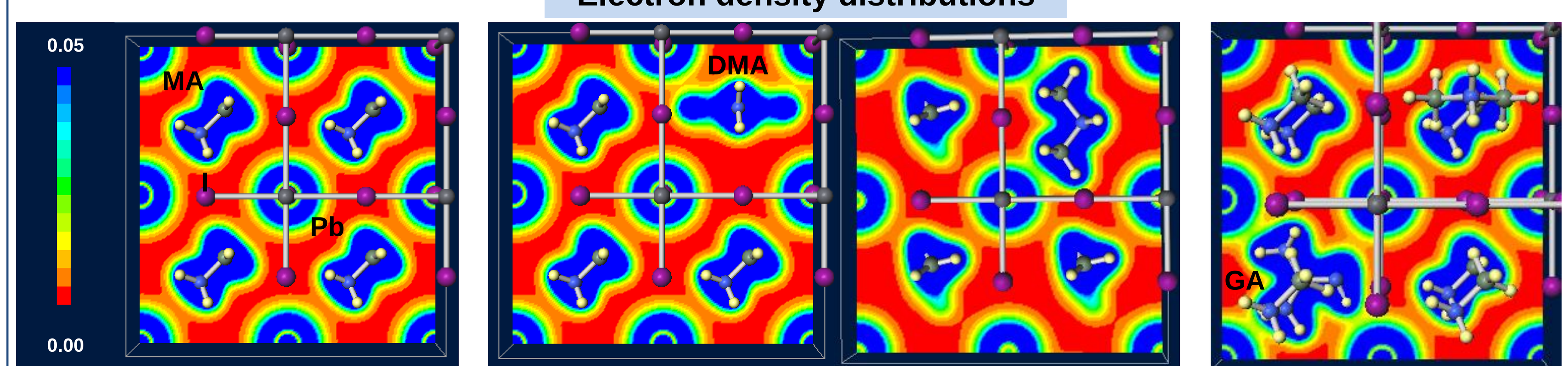

Crystal model	E_{tot} (eV cell^{-1})	E_g (eV)	m^*_e / m_0	m^*_h / m_0
MAPbI$_3$	-3751	1.465	0.298	0.187
MA$_{0.875}$DMA$_{0.125}$PbI$_3$	-3776	1.301	0.298	0.164
MA$_{0.75}$DMA$_{0.25}$PbI$_3$	-3801	1.312	0.268	0.162
MA$_{0.625}$DMA$_{0.375}$PbI$_3$	-3826	1.281	0.273	0.165
MA$_{0.75}$GA$_{0.125}$DMA$_{0.125}$PbI$_3$	-3846	1.312	0.309	0.162

$$\mu = \frac{q\tau}{m^*}$$

μ : carrier mobility

m^* : effective mass

DMA/GA addition

→ Improvement in carrier mobility

Energy level

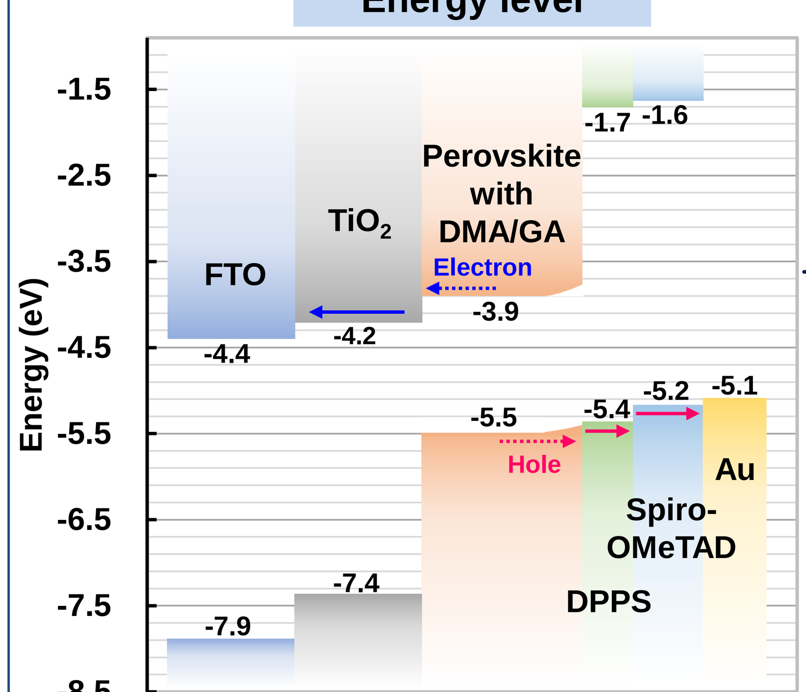

Improvement of interfacial microstructure

・(100) orientation was predominant

→ Enhanced crystal alignment

⇒ Uniform charge transfer (Pvsk/DPPS)

・Larger crystallite size

→ Suppressed carrier recombination

⇒ More efficient carrier transport

・More favorable band bending

・Increase in V_{OC} (experiment)

・Reduction in hole effective mass (calculation)

Born-Oppenheimer molecular dynamics calculations

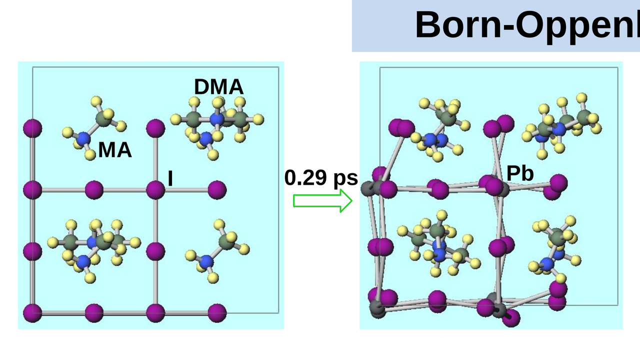

MA$_{0.75}$DMA$_{0.25}$PbI$_3$

Crystal model	300 K				
	E_{tot} (eV cell^{-1}) (1200 step)	D (×10^{-5} cm^2 s^{-1}) C	N	Pb	I
MAPbI$_3$	-3751	1.00	1.95	1.88	3.03
MA$_{0.75}$DMA$_{0.25}$PbI$_3$	-3801	6.35	3.27	1.26	2.15
MA$_{0.75}$DMA$_{0.125}$GA$_{0.125}$PbI$_3$	-3846	4.27	4.27	1.13	2.39

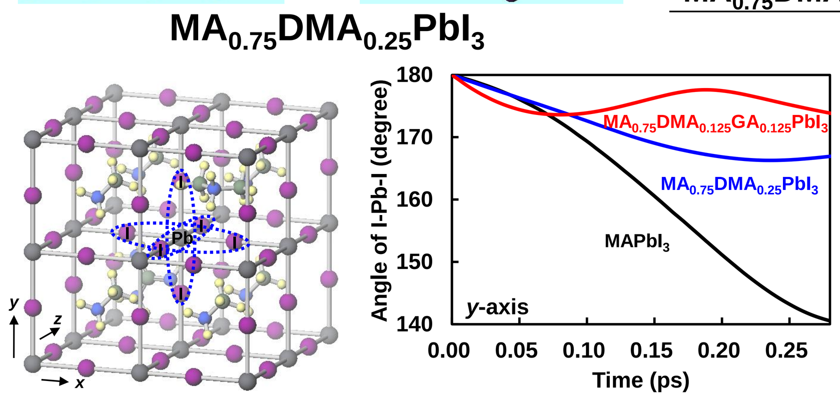

・Decrease in diffusion coefficients (Pb and I around MA and DMA)

→ Stabilization of PbI$_6$ crystal lattice

・DMA/GA co-addition

・Restricted MA mobility

・Formation of hydrogen bonds between H(GA)-I)

→ Suppression of distortion of I-Pb-I angles

Conclusion

Reference: H. Shimada, T. Oku, A. Suzuki, T. Tachikawa, T. Hasegawa, S. Fukunishi, Results in Surfaces and Interfaces (2025) 100528.

・The addition of 30–35% DMA at the MA sites was effective

→ Improved interfacial conditions enhanced the FF, V_{OC}, and η.

・DMA/GA co-addition increased J_{SC} and achieved good stability

→ Larger ionic sizes suppressed MA desorption.

・First-principles calculations revealed reduced total energy, increased carrier mobilities, and lowered diffusion coefficients

→ Emphasized the effectiveness of DMA (and GA) addition.